Bulgarian Chemical Communications, Volume 57, Issue 3 (pp. 170-174) 2025 DOI: 10.34049/bcc.57.GS-MB

In silico insight on hyaluronic acid and boron hyaluronate

G. Serdaroğlu[1*], M. Bolat[2], D. Ali Köse[3], Z. Öztemür[4], N. Karakuş[5]

[1]*Sivas Cumhuriyet University, Faculty of Education, Math. and Sci. Edu., 58140, Sivas, Turkey*
[2]*Hitit University, Vocational School of Technical Sciences, Department of Property Protection and Security, 19900, Çorum, Turkey*
[3]*Hitit University, Faculty of Arts and Sciences, Department of Chemistry, 19040, Çorum, Turkey*
[4]*Sivas Cumhuriyet University, Faculty of Medicine, Department of Orthopedic and Traumatology, 58140, Sivas, Turkey*
[5]*Sivas Cumhuriyet University, Faculty of Science, Department of Chemistry, 58140, Sivas, Turkey*

Accepted: Accepted: August 17, 2025

Hyaluronic acid (HA) and galacturonic acid (GA) core structures and their boron derivatives were investigated using *in silico* tools to predict/elucidate physicochemical and electronic profiles. First, geometry optimization and structural confirmation of the core structures and designed derivatives were performed at B3LYP/6-311G** level. Then, the thermochemistry, lipophilicity, and water solubility properties of the data set were determined to provide the main physicochemical profiles, which would have an essential role in early-stage drug-design research. Further, NBO analyses were performed to evaluate the important intramolecular interactions contributing to lowering of the stabilization energy.

Keywords: Hyaluronic acid, boron hyaluronate, DFT, solubility

INTRODUCTION

Hyaluronic acid, a natural unbranched polymer, is a member of heteropolysaccharides, and pioneering research on HA goes back to the 1880s [1]. HA and related molecular systems are getting increasing attention due to the inclusion of hydroxyl, carboxyl, acetamido, and anomeric carbons, which provide structural advantages [2-4]. The viscoelasticity and hydrophilic nature of these compounds with biocompatible and degradable properties make them very useful in biomedical applications such as regenerative medicine and target-specific therapies [5, 6]. Nowadays, *in silico* investigations provide great advantages in early-stage drug design via saving time and resource consumption in the related processes. In this regard, Azam and co-workers have investigated the adsorption mechanism of methotrexate on hyaluronic acid using DFT and molecular dynamic simulations [7]. Also, the HA-curcumin hybrid compound has been analyzed with NBO and FMO analyses at B3LYP/6-311G(d,p) level to elucidate the electronic structure and possible reactivity features [8]. In a recent work on HA in salt media has been investigated using QM and molecular dynamic simulations to enlighten the hydration and assembly of HA [9]. Wang and co-workers have performed the DFT-D simulations to evaluate the adsorption characteristics of HA onto graphene sheets to explore the possible usage in biomedical applications of graphene-hyaluronic acid (HA) composites [10].

Herein, the quantum mechanical computations were performed to evaluate the physicochemical and electronic properties of HA and the structurally similar GA (galacturonic acid) compounds, their boron-doped derivatives, and Na-salts.

Computational details

The quantum mechanical simulations of the neutral molecules and their Na-salts were performed by the G16W [11] package at B3LYP/6-311G** [12,13] level. The GaussView 6.0.16 [14] package was used to illustrate optimized structures, FMO densities, and MEP plots. The thermochemical data obtained from the simulations were evaluated using the basis of quantum statistical principles [15,16]. Also, the NBO analyses were performed to predict the intramolecular interactions, which contributed to the lowering stabilization energy [17,18].

The HOMO and LUMO energies were used to predict *I* (ionization energy) and *A* (electron affinity) [19]; then, the global reactivity indices were determined using the following equations.

$I = -E_{HOMO}$ and $A = -E_{LUMO}$ $\quad \chi = -(\frac{I+A}{2})$

$\eta = \frac{I-A}{2}$ $\quad \omega = \frac{\mu^2}{2\eta}$ $\quad \Delta N_{max} = (I+A)/2(I-A)$

$\omega^+ \approx (I+3A)^2/(16(I-A))$

$\omega^- \approx (3I+A)^2/(16(I-A))$

$\Delta\varepsilon_{back-donation} = -(\eta/4)$

* To whom all correspondence should be sent:
E-mail: *goncagul.serdaroglu@gmail.com*

wherein the terms are defined as $\chi \rightarrow$ electronic chemical potential $\eta \rightarrow$ global hardness, $\omega \rightarrow$ electrophilicity, $\Delta N_{max} \rightarrow$ maximum charge transfer capability index [20, 21], $\omega^{-} \rightarrow$ electrodonating power, $\omega^{+} \rightarrow$ electroaccepting power [22], and $\Delta E_{back\text{-}donat.} \rightarrow$ back-donation energy [23].

The lipophilicity [24-28] and water-solubility [29,30] properties of the HA and GA derivatives were estimated using SwissADME [31] tools.

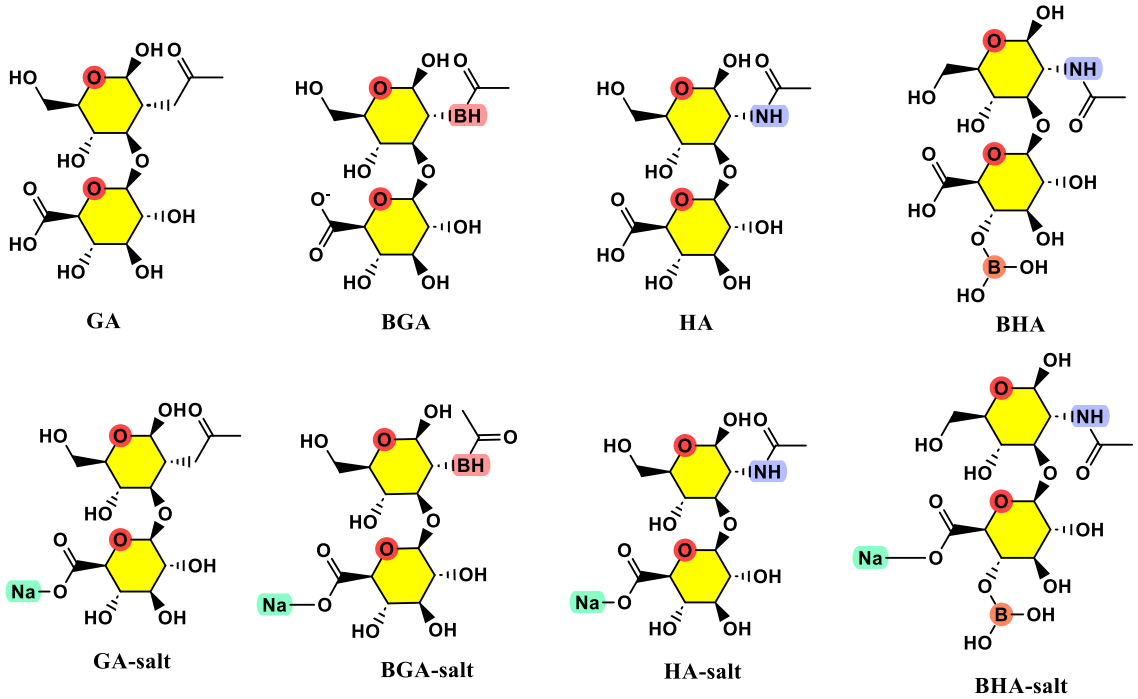

Fig. 1. Optimized chemical structures of the data set

RESULTS AND DISCUSSION

Physicochemistry

The thermochemical and physical parameters of the data set are summarized in Table 1. Accordingly, the ΔE, ΔH, and ΔG quantities of the BHA molecule were determined as -1680.871413, -1680.840013, and -1680.934043 au, respectively, whereas these values of BGA were computed as -1474.851916, -1474.822816, and -1474.911318 au. On the other hand, the BHA (6 D) molecule would have a bigger dipole moment than the others for their neutral forms, while the BGA-salt (11.45 D) would have the biggest dipole moment among the Na-salts. Moreover, the biggest polarizability value was calculated for the BHA and BHA-Na salt at 218.53 and 223.82 au, respectively. Furthermore, Cv and S values of the BHA neutral molecule were determined as 114.690 and 197.903 cal.mol/K, respectively, whereas these values for BHA-Na salt were predicted as 118.828 and 202.230 cal.mol/K. Accordingly, the BHA and BHA-Na systems would have the biggest heat capacity and entropy values for the neutral and salt forms, respectively. From Table 2, the consensus LogPo/w /w order of the neutral structures was calculated as BHA (-4.82)< HA (-3.75)< BGA (-3.48)< GA (-3.39); the boron-doped HA molecule could exhibit less electrophilic character among the compounds, and vice versa for GA molecule. Except for the iLOGP method, the approaches gave the same order as the neutral structures. Herein, the order of the lipophilicity. Also, the BHA and its Na-salt would have the highest solubility in water in comparison to the other molecules, depending on all approaches.

NBO study

Table 3 summarizes the resonance (n→ π*) and anomeric (n→ σ*) interactions of the HA and BHA compounds. Accordingly, the LP (1) N13 (EDi= 1.70010e)→ π* O12-C26 (EDj= 0.29999e) resonance for HA was calculated with the $E^{(2)}$ of 61.99 kcal/mol, which was the highest contribution to the lowering energy. On the other hand, the LP (2) O9 (EDi= 1.80218e)→ π* O10-C24 (EDj= 0.20798e) resonance for the BHA compound would have the biggest contribution to the lowering stabilization energy with $E^{(2)}$ of 48.32 kcal/mol. Also, the LP (1) N2 (EDi= 1.74008e)→ π* O11-C25 (EDj= 0.22282e) and LP (2) O28 (EDi= 1.84202e)→ LP (1) B (EDj= 0.42071e) interactions for BHA compound would have critical role in lowering of the stabilization energy with $E^{(2)}$ of 26.32 and 54.83 kcal/mol, respectively.

Table 1. Thermochemical and physical values of the data set

Comp.	ΔE (au)	ΔH (au)	ΔG (au)	$E_{therm.}$ (kcal/mol)	Cv (cal.mol/K)	S (cal.mol/K)	μ (D)	α (au)
GA	-1488.699821	-1488.670393	-1488.760502	275.808	105.856	189.651	2.97	203.68
BGA	-1474.851916	-1474.822816	-1474.911318	265.955	105.255	186.267	4,85	208.82
HA	-1504.788029	-1504.759238	-1504.847002	269.246	104.287	184.716	3.09	200.53
BHA	-1680.871413	-1680.840013	-1680.934043	287.409	114.690	197.903	6,00	218.53
GA-Na	-1650.493388	-1650.463057	-1650.555644	269.739	108.452	194.865	11.95	214,07
BGA-Na	-1636.620680	-1636.589568	-1636.684508	259.455	109.788	199.818	11.45	216.96
HA-Na	-1666.560761	-1666.530837	-1666.620838	263.169	107.764	189.423	4.58	209.25
BHA-Na	-1842.655690	-1842.623257	-1842.719343	280.396	118.828	202.230	8,24	223.82

Table 2. Lipophilicity and water solubility

	GA	BGA	HA	BHA	GA-salt	BGA-salt	HA-salt	BHA-salt
Lipophilicity								
iLOGP	-3.20	0.00	-0.53	0.00	0.00	0.00	0.00	0.00
XLOGP3	-1.90	-2.26	-3.05	-4.92	-3.09	-2.26	-3.63	-4.61
WLOGP	-4.18	-5.05	-5.31	-6.17	-4.15	-4.99	-5.24	-6.24
MLOGP	-3.45	-4.12	-4.46	-5.85	-3.77	-4.12	-4.37	-5.85
SILICOS-IT	-4.23	-5.99	-5.37	-7.15	-4.63	-7.30	-5.76	-8.23
Avg. LogPo/w	-3.39	-3.48	-3.75	-4.82	-3.13	-3.73	-3.80	-4.99
Water Solubility								
Log S (ESOL)	-0.84	-0.53	-0.05	1.05	-0.02	-0.67	0.31	0.79
Solubility (mg/mL)x10^2	0.578	1.16	3.53	49.8	3.95	0.898	8.54	28.4
Class	VS	VS	VS	HS	VS	VS	HS	HS
Log S (Ali)	-1.85	-1.48	-0.91	0.41	-0.39	-1.41	-0.08	0.32
Solubility (mg/mL)x10^2	0.0558	0.131	0.488	11.4	1.72	0.161	3.50	9.68
Class	VS	VS	VS	HS	VS	VS	VS	HS
Log S (SILICOS-IT)	2.80	3.16	3.16	4.62	3.06	3.11	3.41	4.25
Solubility (mg/mL)x10^5	2.51	5.75	5.69	183	4.80	5.32	10.9	82.4
Class	S	S	S	S	S	S	S	S

Table 3. NBO analysis results of the possible interactions

	Donor(i)	ED_i/e	Acceptor(j)	ED_j/e	$E^{(2)}$ kcal/mol	E(j)-E(i)/a.u	F(i.j)/a.u
HA	LP (2) O1	1.88758	σ* O3-C18	0.07364	15.92	0.58	0.086
	LP (2) O5	1.93345	σ* O2-C19	0.05344	11.01	0.62	0.074
	LP (2) O10	1.81638	π* O11-C25	0.19386	45.33	0.35	0.113
	LP (2) O11	1.84432	σ* C23-C25	0.07228	19.97	0.62	0.102
	LP (2) O12	1.87173	σ* N13-C26	0.07297	23.65	0.73	0.119
			σ* C26-C27	0.05406	18.46	0.63	0.098
	LP (1) N13	1.70010	π* O12-C26	0.29999	61.99	0.29	0.120
BHA	LP (2) O1	1.89101	σ* O3-C17	0.06881	14.05	0.58	0.082
	LP (2) O5	1.93075	σ* O2-C18	0.05813	12.71	0.61	0.079
	LP (2) O7	1.85047	LP(1) B	0.42071	39.55	0.33	0.109
	LP (2) O9	1.80218	π* O10-C24	0.20798	48.32	0.35	0.116
	LP (2) O10	1.85191	σ* C22-C24	0.07128	18.24	0.63	0.098
	LP (2) O11	1.86932	σ* N12-C25	0.06877	20.75	0.72	0.111
			σ* C25-C26	0.05191	18.83	0.65	0.101
	LP (1) N2	1.74008	π* O11-C25	0.22282	26.32	0.38	0.090
	LP (2) O28	1.84202	LP(1) B	0.42071	54.83	0.31	0.124

FMO and MEP analyses

The reactivity values obtained from FMOs' energies have been used to predict the possible reactivity directions and regions of the molecular systems, wherein the determined reactivity values of the compounds change in the following orders of

ΔE (L-H): HA (6.733)> BHA (5.94)> GA (5.88)> BGA (5.144)> BHA-salt (5.25)> HA-salt (4.945) > GA-salt (4.185)> BGA-salt (4.034)

μ: BGA (–4.316)< BHA-salt (–4.276)< BHA (–4.251)< GA-salt (–4.106)< BGA-salt (–4.025)< HA (–3.803)< HA-salt (–3.786)< GA (–3.672)

η: HA (3.366)> BHA (2.97)> GA (2.94)> BHA-salt (2.625)> BGA (2.572)> HA-salt (2.473)> GA-salt (2.092)> BGA-salt (2.017)

ω: BGA-salt = GA-Salt (0.148)> BGA (0.133)> BHA-salt (0.128)> BHA (0.112)> HA-salt (0.107)> GA (0.084)> HA (0.079)

ω^+: BGA-salt (0.083)> GA-salt (0.082)> BGA (0.066)> BHA-salt (0.061)> HA-salt (0.048)> BHA (0.047)> GA (0.030)> HA (0.025)

ω^-: GA-salt (0.233)> BGA-salt (0.231)> BGA (0.224)> BHA-salt (0.219)> BHA (0.204)> HA-salt (0.187)> GA (0.165)> HA (0.164)

ΔN_{max}: BGA-salt (1.996)> GA-salt (1.962)> BGA (1.678)>BHA-salt (1.629)> HA-salt (1.531)> BHA (1.431)> GA (1.249)> HA (1.130)

$\Delta E_{back.}$: HA (–0.842)< BHA (–0.742)< GA (–0.735)< BHA-salt (–0.656)< BGA (–0.643)< HA-salt (–0.618)< GA-salt (–0.523)< BGA-salt (–0.504)

Table 4. Chemical reactivity parameters

	H (-I)/ eV	L (-A)/ eV	ΔE (L-H)/ eV	μ/ eV	η/ eV	ω/ au	ω^+/ au	ω^-/ au	ΔN_{max}/ eV	$\Delta E_{back.}$/ eV
GA	-6,612	-0,732	5,880	-3,672	2,94	0,084	0,03	0,165	1,249	-0,735
BGA	-6,888	-1,744	5,144	-4,316	2,572	0,133	0,066	0,224	1,678	-0,643
HA	-7,17	-0,437	6,733	-3,803	3,366	0,079	0,025	0,164	1,13	-0,842
BHA	-7,221	-1,281	5,940	-4,251	2,97	0,112	0,047	0,204	1,431	-0,742
GA-Salt	-6,198	-2,014	4,185	-4,106	2,092	0,148	0,082	0,233	1,962	-0,523
BGA-salt	-6,042	-2,008	4,034	-4,025	2,017	0,148	0,083	0,231	1,996	-0,504
HA-salt	-6,259	-1,313	4,945	-3,786	2,473	0,107	0,048	0,187	1,531	-0,618
BHA-Salt	-6,901	-1,651	5,250	-4,276	2,625	0,128	0,061	0,219	1,629	-0,656

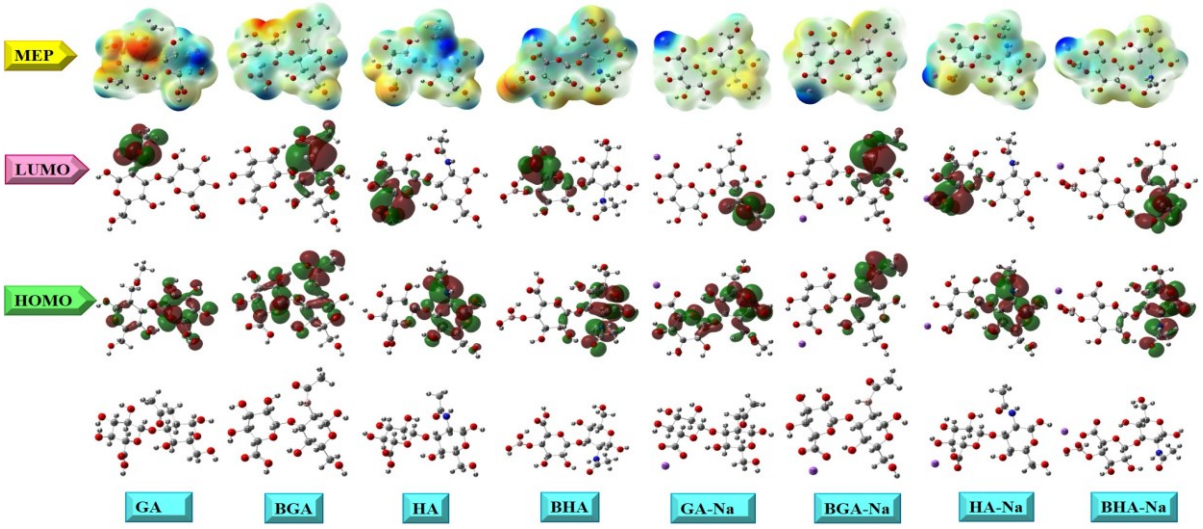

Fig. 2. Optimized structures. HOMO. LUMO. and MEP diagrams of the data set

From Table 4, the HA molecule, in comparison to the other molecules, would prefer to interact with the outer system rather than the intramolecular charge transition between the FMOs due to having the highest energy gap value (ΔE_{L-H}=6.733 eV), and vice versa for BGA-salt. The results revealed that the HA molecule would exhibit the hardest character (η=3.366 eV), less charge transfer capability (ΔN_{max}=1.130 eV), and could gain more stabilization via back donation ($\Delta E_{back.}$=–0.842 eV) than the others could. On the other hand, the BGA-salt structure would be softer (η=2.017 eV) than the others, as well as having the highest charge transfer capability (ΔN_{max}=1.996 eV) and less stabilization via back donation ($\Delta E_{back.}$=–0.504 eV). Figure 2 displays the FMOs' densities and MEP plots of the

dataset. As expected, the H atom(s) belonging to the -OH group were covered by blue color (V>0) as an indicator of the electron-poor region for the nucleophiles as a function of the electrostatic potential, whereas the O atom of the carboxyl group was covered by red (V<0) as a marker of the electron-rich region for the electrophiles. The HOMO for the GA was expanded on carboxylic acid substituted ring (right) mostly and slightly other ring, whereas the LUMO was densified on the -butan-2-one substitution. On the other hand, the HOMO for HA and BHA molecules was separated on the acetamide-substituted ring mostly, whereas the LUMO appeared on the other ring (left) substituted by carboxylic acid substituted.

CONCLUSION

Herein the HA and the structurally similar GA main compounds and their boron derivatives were investigated using computational tools. The B3LYP/6-311G** level computations were performed to predict/evaluate the optimized structures, thermochemistry, NBO and FMO analyses. SwissADME online tools were used to determine the solubility features in octanol and water, which would help to provide insight into early-stage drug-design works.

Acknowledgement: *All calculations have been carried out at TUBITAK ULAKBIM, High Performance and Grid Computing Center (TR-Grid e-Infrastructure). The author thanks the Scientific Research Projects Department of Cumhuriyet University (Project No: EĞT-2024-099).*

REFERENCES

1. G. Abatangelo, V. Vindigni, G. Avruscio, L. Pandis, P. Brun, *Cells,* **9**(7), 1743 (2020).
2. A. Fallacara. E. Baldini. S. Manfredini, S. Vertuani, *Polymers*, **10**(7), 701 (2018).
3. J. Necas, L. Bartosikova, P. Brauner, J. Kolar, *Veterinarni Medicina,* **53**(8), 397 (2008).
4. N.M. Salwowska, K.A. Bebenek, D.A. Żądło, D.L. Wcisło-Dziadecka, *J. Cosmet. Dermatol*., **15**, 520 (2016).
5. H. Pereira, D.A. Sousa, A. Cunha, R. Andrade, J. Espregueira-Mendes, J.M. Oliveira, R.L. Reis, in: J. Oliveira, S. Pina, R. Reis, J. San Roman (eds.). Osteochondral Tissue Engineering. Adv. Exp. Med. Biol., vol. 1059. Springer. Cham., 2018, p. 139.
6. R.D. Price, M.G. Berry, H.A. Navsaria, *J. Plast. Reconstr. Aesthet. Surg.,* **60**(10), 1110 (2007).
7. F. Azam, H.R. Abd El-Mageed, M.J. Anwar, D. Mahmood, *Chem. Phys. Impact*., **8**, 100573 (2024).
8. S.A.K. Kirmani, P. Ali, F. Azam, A.E. Kuznetsov, P.A. Alvi, *Comput. Theor. Chem*., **1214**, 113761 (2022).
9. S. Vasudevan, S. Chattaraj, A. Enrico, F.S. Pasqualini, *Langmuir,* **41**(6), 3852 (2025).
10. Q. Wang, W. She, X. Lu, P. Li, Y. Sun, X. Liu, W. Pan, K. Duan, *Comput. Theor. Chem.*, **1165**,112559 (2019).
11. A. D. Becke, *J. Chem. Phys*., **98**, 1372 (1993).
12. C. Lee, W. Yang, R.G. Parr, *Phys. Rev*., **B37**, 785 (1988).
13. M. J. Frisch et al. Gaussian 09W. Revision D.01. Gaussian. Inc. Wallingford CT. 2013.
14. GaussView 6.0.16. Gaussian. Inc. Wallingford CT. (2016).
15. D. A. McQuarrie, Statistical Thermodynamics. Harper & Row Publishers. New York, 1973.
16. G. Serdaroglu, S. Durmaz, *Indian J. Chem*., **49**, 861 (2010).
17. J.P. Foster, F. Weinhold, *J. Am. Chem. Soc*., **102**, 7211 (1980).
18. A.E. Reed, L.A. Curtiss, F. Weinhold, *Chem. Rev*., **88**, 899 (1988).
19. T. Koopmans, *Physica*, **1**, 104 (1934).
20. R. G. Pearson, *Proc. Natl. Acad. Sci. USA*., **83**, 8440 (1986).
21. R. G. Parr, L.V. Szentpaly, S. Liu, *J. Am. Chem. Soc*., **121**, 1922 (1999).
22. J. L. Gazquez, A. Cedillo, A. Vela, *J. Phys. Chem. A*., **111**(10), 1966 (2007).
23. B. Gomez, N. V. Likhanova, M. A. Domínguez-Aguilar, R. Martínez-Palou, A. Vela, J. L. Gazquez, *J. Phys. Chem. B.,* **110**(18), 8928 (2006).
24. A. Daina, O. Michielin, V. Zoete, *J. Chem. Inf. Model*. **54**(12), 3284 (2014).
25. T. Cheng, Y. Zhao, X. Li, F. Lin, Y. Xu, X. Zhang, Y. Li, R. Wang, *J. Chem. Inf. Model*., **47**(6), 2140 (2007).
26. S. A. Wildman, G. M. Crippen, *J. Chem. Inf. Comput. Sci.,* **39**, 868 (1999).
27. C. A. Lipinski, F. Lombardo, B. W. Dominy, P. J. Feeney, *Adv. Drug Deliver. Rev*., **46**, 3 (2001).
28. Silicos-IT. [Online]. Available: https://www.silicos-it.be.
29. J. S. Delaney, *J. Chem. Inf. Comput. Sci*.. **44**, 1000 (2004).
30. J. Ali, P. Camilleri, M. B. Brown, A. J. Hutt, S. B. Kirton, *J. Chem. Inf. Model*., **52**, 2950 (2012).
31. A. Daina, O. Michielin, V. Zoete, *Sci Rep*., **7**, 42717 (2017).